Russian Chemical Bulletin, International Edition, Vol. 69, No. 4, pp. 647—652, April, 2020

Full Articles

Mechanism of CO oxidation by oxygen in the presence of palladium(II) bromide complexes: a quantum chemical modeling

R. S. Shamsiev

MIREA — Russian Technological University, M. V. Lomonosov Institute of Fine Chemical Technologies,
86 prosp. Vernadskogo, 119571 Moscow, Russian Federation.
Fax: +7 (495) 434 9287. E-mail: Shamsiev.R@gmail.com

Mechanisms of CO oxidation by oxygen in the $PdBr_2$—LiBr—MeCN—H_2O system in the absence and in the presence of iron(II) phthalocyaninate (PcFe) as co-catalyst were studied within the framework of the density functional theory with the PBE functional. According to calculations, palladium(II) bromide complexes most likely occur as $Pd(AN)(CO)Br_2$ (AN is acetonitrile), $Pd(CO)_2Br_2$, and $[Pd(CO)Br_3]^-$. From the results of calculations it follows that neutral complexes $Pd(AN)(CO)Br_2$ and $Pd(CO)_2Br_2$ can be highly catalytically active in the CO oxidation. Insertion of O_2 into the Pd—H bond in the hydride complexes is the rate-limiting step of the CO oxidation reaction proceeding in the absence of PcFe as co-catalyst. Iron(II) phthalocyaninate present in the reaction system causes a noticeable decrease in the activation energy of regeneration of the Pd^{II} complexes due to more efficient activation of O_2. The oxidation of palladium hydride complexes by iron superoxophthalocyaninate can follow two routes that differ in the fashion of hydride transfer.

Key words: CO oxidation, iron phthalocyaninate, palladium complexes, catalyst turnover frequency (TOF), energetic span model, density functional theory.

Oxidative carbonylation of alkynes has long been known in metal complex catalysis and well documented in reviews[1—5] and monographs.[6—8] Among practically important oxidative carbonylation reactions of acetylene (and alkynes), there is oxidative dicarbonylation affording maleic anhydride (MA) and suitable for the synthesis of doubly ^{13}C-labeled MA. Such compounds are widely used in medical diagnosis.[9] The reaction proceeds efficiently in the catalytic system $PdBr_2$—LiBr—MeCN—H_2O. To reduce the partial pressure of oxygen, metal phthalocyaninates (PcM) are used as co-catalysts[10] for O_2 activation. The synthesis of MA is accompanied by the oxidation of CO and formation of succinic anhydride as side processes.[11] An experimental study of the CO oxidation in these systems[12] was motivated by the following reasons. First of all, the mechanism of this "simple" process involves two "blocks" of reaction steps that are common to the oxidation of CO and the synthesis of MA. These are (i) the formation of Pd^{II} hydroxycarbonyl and hydride complexes[11—13] and (ii) PcM-catalyzed (M = Mn, Fe,

Published in Russian in *Izvestiya Akademii Nauk. Seriya Khimicheskaya,* No. 4, pp. 0647—0652, April, 2020.

Co) and non-catalyzed oxidation of the hydride and other reduced forms of Pd^{II} by oxygen.[10—12] Besides, elucidation of factors influencing the rate of CO oxidation (concentrations of water, LiBr, and PcM) is of importance for searching ways to improve the selectivity of MA synthesis with respect to ^{13}CO consumption. Understanding of the mechanism of this simple catalytic reaction is also of importance for optimizing the MA synthesis conditions and for the development of theory of homogeneous oxidation reactions in metal complex catalysis. Therefore, the aim of this work is to carry out a quantum chemical modeling of the mechanisms of CO oxidation by oxygen in the absence and in the presence of iron(II) phthalocyaninate as co-catalyst.

Calculation Methods

Calculations were mainly carried out within the framework of the density functional theory in the all-electron scalar-relativistic approximation using the Priroda program,[14,15] the PBE exchange-correlation functional,[16] and the L11 all-electron basis set.[17] This technique was previously used in modeling of the mechanisms of ethylene oxidation on palladium complexes[13] and propionic acid deoxygenation on palladium clusters.[18] Results for open-shell systems were obtained from spin-polarized DFT calculations. Anionic complexes of palladium were calculated taking into account the presence of counterion(-s), *viz.*, a Li atom solvated by three acetonitrile (AN) molecules and one water molecule $[Li(AN)_3(H_2O)]^+$. The types of the optimized structures were confirmed by vibrational frequency analysis. Thermodynamic parameters (ΔG_{298}, $\Delta G^{\neq}{}_{298}$) were calculated for $T = 298$ K. The turnover frequency (TOF) of the catalyst in each pathway was calculated using the energetic span model[19] and the results of quantum chemical modeling.

Results and Discussion

On the state of Pd^{II} complexes in acetonitrile. Palladium(II) bromide complexes in AN can exist as binuclear complex $Pd_2(AN)_2Br_4$.[20] Results of our calculations of changes in the Gibbs energy (Δ_rG_{298}) in different decomposition reactions of $Pd_2(AN)_2Br_4$ are included in the description of the set of reactions (*1*)—(*10*). The Δ_rG_{298}/kcal mol^{-1} values are given in parentheses near the reaction equation; the values calculated taking account of counterions are asterisked. The data showed that the binuclear complex is in equilibrium with the mononuclear complex $Pd(AN)_2Br_2$ (reaction (*1*)). The decay of $Pd_2(AN)_2Br_4$ into an ion pair composed of complexes $[Pd(AN)_3Br]^+$ and $[Pd(AN)Br_3]^-$ is thermodynamically forbidden (reaction (*2*)). The binuclear complex can decompose into complexes $Pd(AN)_2Br_2$ and $[Pd(AN)Br_3]^-$ in the presence of bromide ions (reaction (*3*)) and undergo irreversible decomposition into $Pd(CO)(AN)Br_2$ and $Pd(AN)_2Br_2$ in the presence of CO molecules (reaction (*4*)).

$Pd_2(AN)_2Br_4 + 2\ AN = 2\ Pd(AN)_2Br_2$ (0.3) (*1*)

$Pd_2(AN)_2Br_4 + 2\ AN =$
$= [Pd(AN)_3Br][Pd(AN)Br_3]$ (20.2) (*2*)

$Pd_2(AN)_2Br_4 + AN + Br^- =$
$= Pd(AN)_2Br_2 + [Pd(AN)Br_3]^-$ (–6.8)* (3)

$Pd_2(AN)_2Br_4 + AN + CO =$
$= Pd(AN)(CO)Br_2 + Pd(AN)_2Br_2$ (–12.6) (*4*)

$Pd(AN)_2Br_2 + CO = Pd(AN)(CO)Br_2 + AN$ (–13.0) (*5*)

$[Pd(AN)Br_3]^- + CO = [Pd(CO)Br_3]^- + AN$ (–16.4)* (*6*)

$Pd(AN)(CO)Br_2 + CO = Pd(CO)_2Br_2 + AN$ (0.4) (*7*)

$[Pd(CO)Br_3]^- + CO = Pd(CO)_2Br_2 + Br^-$ (14.8)* (*8*)

$Pd(AN)_2Br_2 + Br^- = [Pd(AN)Br_3]^- + AN$ (–11.3)* (*9*)

$Pd(AN)_2Br_2 + H_2O = Pd(AN)(H_2O)Br_2 + AN$ (4.2) (*10*)

The substitution of AN by CO in the mononuclear complexes $Pd(AN)_2Br_2$ and $[Pd(AN)Br_3]^-$ is energetically favorable since the Gibbs energy decreases by 13.0 and 16.4 kcal mol^{-1}, respectively (reactions (*5*) and (*6*)). However, subsequent exchange of the AN ligand in $Pd(CO)(AN)Br_2$ or Br ligands in $[Pd(CO)Br_3]^-$ by CO is energetically unfavorable (reaction (*7*)) or forbidden (reaction (*8*)). We also found that substitution of AN ligand in $Pd(AN)_2Br_2$ by bromide ion (reaction (*9*)) is thermodynamically favorable, while the replacement by H_2O (reaction (*10*)) is unfavorable.

Thus, the binuclear complex $Pd_2(AN)_2Br_4$ is stable only in acetonitrile. Carbon monoxide molecules or bromide ions present in the reaction system cause irreversible decomposition of $Pd_2(AN)_2Br_4$ into mononuclear complexes. In this connection, it seems reasonable to consider only mononuclear Pd^{II} complexes, *viz.*, $Pd(AN)(CO)Br_2$ (**1**), $Pd(CO)_2Br_2$ (**2**), and $[Pd(CO)Br_3]^-$ (**3**) as catalytically active species when studying the mechanism of CO oxidation.

Mechanism of CO oxidation in the presence of oxygen. The first "block" of reaction steps in the mechanism of carbon monoxide oxidation involves a two-step transformation of CO to CO_2.[3,8,11,12] It begins with the nucleophilic attack of water molecule on the CO ligand and results in hydroxycarbonyl intermediate $[PdL(COOH)Br_2]^-$ (L = AN (**4**), CO (**5**), Br^- (**6**)). According to calculations, the outer-sphere attack of H_2O molecule on CO is a fairly fast process since the Gibbs activation energy for the formation of intermediates **4—6** varies in the range of 6.6—12.9 kcal mol^{-1}. The process is characterized by low activation barriers only if three water molecules are involved. We failed to locate an energy minimum corresponding to the product formed at this reaction step using one H_2O molecule or one H_2O molecule solvated by two AN molecules. Besides, the experimental results obtained at a LiBr : $PdBr_2$ ratio of 2 used in the synthesis of MA also showed that the rate of CO_2 formation abruptly increases as the water concentration increases by a factor of 1.75 only.[12] The appearance of three water molecules in the transition state of formation of intermediates **4—6** can be explained by successive coordination of water molecules bound to the Br ligand through a hydrogen bond. A similar situation also occurs in the Wacker oxidation mechanism.[13,21—23] A quasi-equilibrium dissociation of palladium aqua complex resulting in [Pd](CO)(OH) can most likely be ruled out because the synthesis of succinic anhydride from CO, H_2O, and C_2H_2, which involves the same step of formation of hydroxycarbonyl complex, proceeds with a kinetic isotope effect close to 1.[11]

The second step is elimination of CO_2 from the hydroxycarbonyl intermediates **4—6** to give the hydride complexes $[Pd(L)(H)Br_2]^-$, where L = AN (**7**), CO (**8**) and Br^- (**9**). It proceeds with a considerable exothermic effect, but involves higher activation barriers compared to the first reaction step. For instance, elimination of CO_2 from complex **5** is characterized by the highest barrier of 28.7 kcal mol^{-1} (*cf.* 9.9 and 15.2 kcal mol^{-1} for complexes **1** and **3**, respectively). These values suggest that elimination of CO_2 from intermediate **5** is nearly unattainable and only two hydride complexes, $[Pd(AN)(H)Br_2]^-$ (**7**) and $[Pd(H)Br_3]^{2-}$ (**9**), can form in the course of the CO oxidation. However, ligand exchange is possible, *e.g.*, substitution of AN by CO in the reaction

$$\underset{\mathbf{7}}{[Pd(AN)(H)Br_2]^-} + CO = \underset{\mathbf{8}}{[Pd(CO)(H)Br_2]^-} + AN$$

is a thermodynamically favorable process ($\Delta_r G°_{298}$ = = –7.3 kcal mol^{-1}).

The next "block" of steps in the reaction mechanism involves the oxidation of the hydride complexes **7—9** by oxygen and their return to the new catalytic cycle in the form of Pd^{II} complexes.[23,24] According to our calculations, these steps in the reaction mechanism can be described by Scheme 1.

Scheme 1

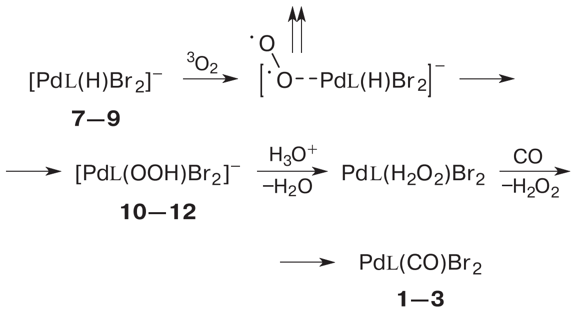

L = AN, CO, Br^-

The primary interaction of O_2 molecule with the palladium atom along the fifth coordinate in the hydride intermediates **7—9** results in van der Waals complexes with Pd—O distances of 2.59 (**7**), 3.05 (**8**) and 2.38 Å (**9**). No structures corresponding to the pre-reaction complexes Pd...H—O_2 described earlier[23,24] were located. Then, the O_2 molecule is inserted into the Pd—H bond of the hydride complex to give palladium hydroperoxide $PdL(OOH)Br_2$ (L = AN (**10**), CO (**11**), Br^- (**12**)). This step is characterized by a moderately high activation barrier ($\Delta G^{\neq}_{298}$ = = 14.9—16.8 kcal mol^{-1}). The formation of hydroperoxides **10—12** is accompanied by a decrease in the spin multiplicity of the complexes from triplet to singlet. Next, intermediates **10—12** undergo barrierless protonation and a H_2O_2 molecule is formed in the coordination sphere of palladium. Eventually, substitution of hydrogen peroxide by CO ligand affords the Pd^{II} complexes **1—3**.

Figure 1 presents the energy diagrams of the reaction of CO oxidation in the presence of complexes **1—3**. It follows that the most active catalyst is the acetonitrile complex **1** for which the maximum Gibbs activation energy is 15.1 kcal mol^{-1} (*cf.* 28.7 and 21.2 kcal mol^{-1} for the pathways involving complexes **2** and **3**, respectively).

Since the Gibbs energies of the following pairs of complexes: **1** and **2**, **5** and **6**, **8** and **9**, **11** and **12** are close, one can assume that an equilibrium between the complexes is established through ligand exchange. In this case one can distinguish five independent routes in the mechanism of CO oxidation (Scheme 2, Table 1).

Scheme 2

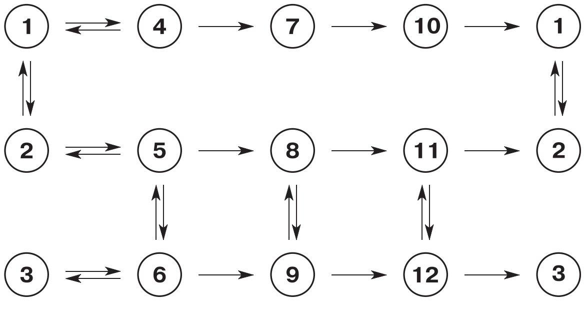

To a first approximation the TOF values for three pathways involving complexes **1—3** can be evaluated ignoring transitions between these pathways. Our TOF calculations (see Table 1) showed that only pathway I catalyzed by complex **1** is important to the reaction mechanism. The transition state of O_2 insertion into the

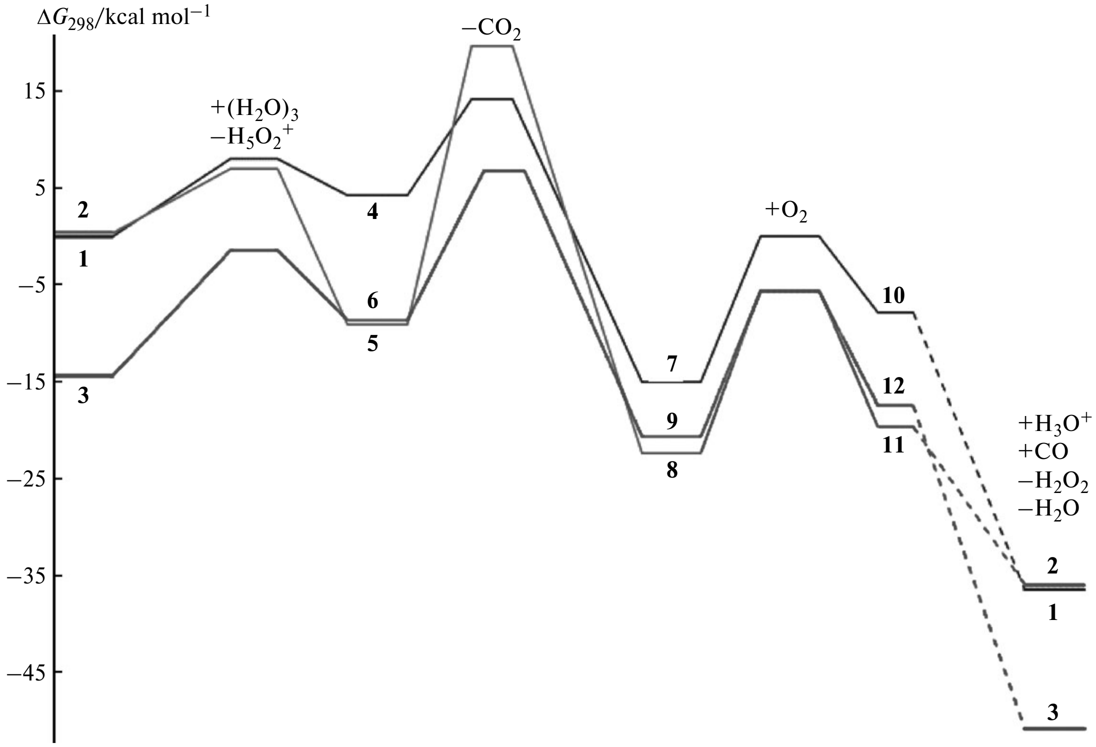

Fig. 1. Energy diagrams of the CO oxidation reaction catalyzed by complexes **1**—**3**.

Pd—H bond is the TOF-determining transition state (TDTS, see Ref. 19) for pathway I. The nature of the rate-limiting steps for pathways I — III is determined by the contributions of the $\Delta G^{\neq}{}_{298}$ values corresponding to CO_2 elimination and the ΔG_{298} values corresponding to the formation of palladium hydride complexes **7**—**9** (complexation of palladium) to the overall rate of the catalytic reaction of CO oxidation.

Taking account of the equilibria $\mathbf{5} \leftrightarrows \mathbf{6}$ and $\mathbf{9} \leftrightarrows \mathbf{8}$, two more pathways, IIa and IIb catalyzed by complex **2**, can be distinguished. The corresponding TOF values (see Table 1) are 8.2 and 2.6 s^{-1}, being much higher than the TOF value for the pathway II involving complex **2**. This suggests that the equilibria $\mathbf{5} \leftrightarrows \mathbf{6}$ and $\mathbf{9} \leftrightarrows \mathbf{8}$ are of importance for the rate of CO oxidation:

$$\mathbf{5} + Br^- = \mathbf{6} + CO,$$

$$\mathbf{9} + CO = \mathbf{8} + Br^-.$$

Besides, an excess of bromide ions ($[Br^-]/[Pd] \geqslant 3$) in the reaction system should facilitate the ligand exchange reactions $\mathbf{1} \leftrightarrows \mathbf{3}$ and $\mathbf{2} \leftrightarrows \mathbf{3}$ and thus cause a noticeable decrease in the rate of CO oxidation since the TOF for pathway III catalyzed by complex **3** is very low (see Table 1):

$$\mathbf{1} + Br^- = \mathbf{3} + AN,$$

$$\mathbf{2} + Br^- = \mathbf{3} + CO.$$

Role of iron(II) phthalocyaninate in the oxidation of palladium hydride complexes. From the energy diagrams (see Fig. 1) and TOF values (see Table 1) it follows that insertion of O_2 into the Pd—H bond in the hydride complexes **7** and **8** can be the rate-limiting step of the CO oxidation provided that the catalyst is involved in complex formation. Clearly, the activation barriers to the insertion of O_2 into the Pd—H bond are due to weak interaction of $^3O_2$ with Pd^{II} in the hydride complexes. More efficient

Table 1. Activation parameters ($\Delta G^{\neq}{}_{298}$) and TOF values for different pathways of the CO oxidation reaction

Pathway	$\Delta G^{\neq}{}_{298}$/ kcal mol^{-1}	TOF/s^{-1}	TDTS
$\mathbf{1} \rightleftarrows \mathbf{4} \longrightarrow \mathbf{7} \longrightarrow \mathbf{10} \longrightarrow \mathbf{1}$ (I)	15.1	44.0	$+O_2$
$\mathbf{2} \rightleftarrows \mathbf{5} \longrightarrow \mathbf{8} \longrightarrow \mathbf{11} \longrightarrow \mathbf{2}$ (II)	28.7	$5.5 \cdot 10^{-9}$	$-CO_2$
$\mathbf{3} \rightleftarrows \mathbf{6} \longrightarrow \mathbf{9} \longrightarrow \mathbf{12} \longrightarrow \mathbf{3}$ (III)	21.2	$1.9 \cdot 10^{-3}$	$-CO_2$
$\mathbf{2} \rightleftarrows \mathbf{5} \longrightarrow \mathbf{6} \longrightarrow \mathbf{9} \longrightarrow \mathbf{12} \rightleftarrows \mathbf{11} \longrightarrow \mathbf{2}$ (IIa)	15.9	8.2	$-CO_2$
$\mathbf{2} \rightleftarrows \mathbf{5} \longrightarrow \mathbf{6} \longrightarrow \mathbf{9} \rightleftarrows \mathbf{8} \longrightarrow \mathbf{11} \longrightarrow \mathbf{2}$ (IIb)	16.7	2.6	$+O_2$

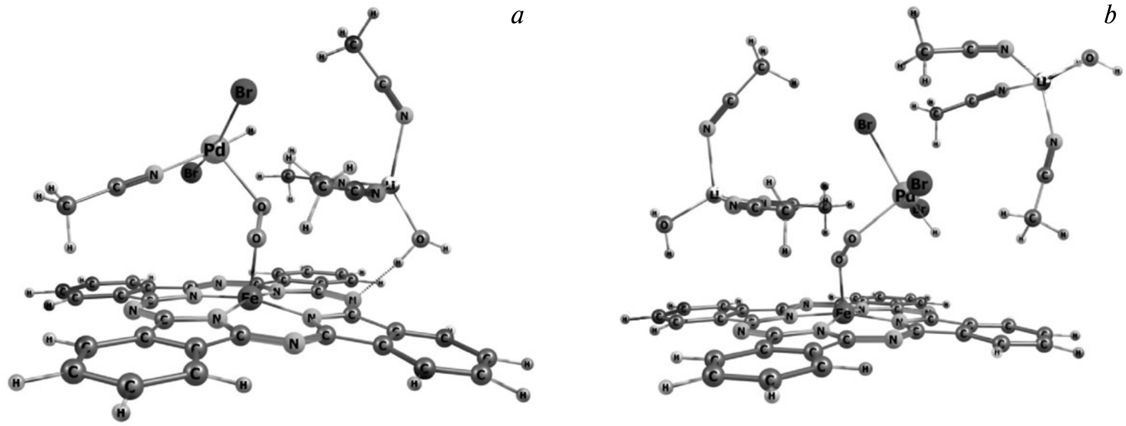

Fig. 2. Optimized structures of μ^2-oxo complexes **7-Pc** (*a*) and **9-Pc** (*b*).

activation of O_2 molecule can be achieved using metal phthalocyaninates, which results in corresponding superoxophthalocyaninates.[25]

According to calculations, the interaction of singlet $PcFe(O_2)$ with the hydride complexes **7** and **9** leads to formation of μ^2-oxo complexes **7-Pc** and **9-Pc** with the —Fe—O—O—Pd— fragment (Fig. 2). Subsequent decomposition of this fragment can follow two routes. One of these is presented for complex **9** in Scheme 3. The key step in this mechanism is the hydride transfer from the Pd atom to the O atom, which leads to dissociation of the O—O bond and formation of complex Pd^{II}—$[Pd(OH)Br_3]^{2-}$ and iron(IV) oxophthalocyaninate. Protonation of palladium hydroxide and substitution of H_2O by CO ligand returns complex **3** to the catalytic cycle. In turn, triplet oxophthalocyaninate PcFe=O is reduced in the reaction with CO with a Gibbs activation energy of 16.9 kcal mol^{-1} (Fig. 3).

Scheme 3

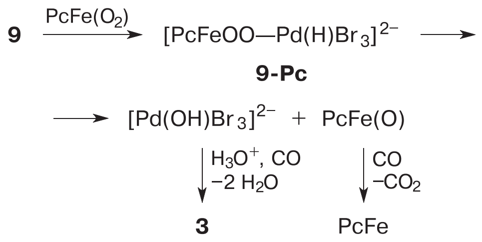

Modeling of the interaction between $PcFe(O_2)$ and the hydride complexes **7** and **8** disclosed the second possible decomposition route of $PcFeOO—PdL(H)Br_2$, where L = AN, CO (Scheme 4). In this case, hydride transfer proceeds with dissociation of the Pd—O bond and formation of iron hydroperoxide $[PcFe(OOH)]^-$, while the O—O bond remains untouched.

Scheme 4

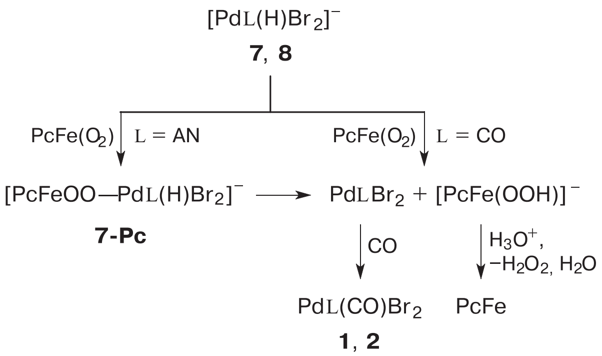

Table 2 lists the activation parameters for the oxidation of palladium hydride complexes **7**—**9** by oxygen in the absence and in the presence of PcFe. It follows that the presence of iron(II) causes a noticeable decrease (by 2—8 kcal mol^{-1}) in the activation energy of the oxidation of hydride complexes **7**—**9**. Therefore, $PcFe(O_2)$ more efficiently regenerates palladium complexes compared to O_2. In addition, the return of Pd^{II} complexes to the catalytic cycle is no longer the rate-limiting step of the pathways catalyzed by complexes **1** and **2**. Therefore, the concentration of oxygen should not significantly influence the rate of CO oxidation.

Summing up, we for the first time carried out a quantum chemical modeling of the reaction of CO oxidation by oxygen the results of which provide further insight into

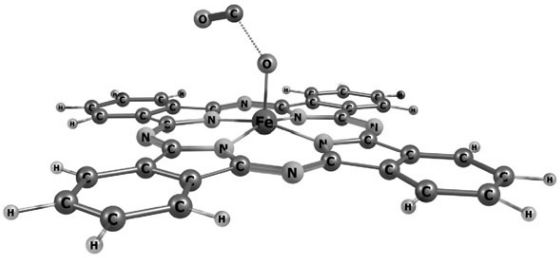

Fig. 3. Optimized TS structure for the stage PcFeO + CO → → PcFe + CO_2.

Table 2. Gibbs activation energy ($\Delta G^{\neq}{}_{298}$/kcal mol^{-1}) of the oxidation of hydride complexes **7**—**9** by oxygen in the absence and in the presence of PcFe

Hydride complex Pd	O_2	O_2/PcFe
7	15.1	13.7
8	16.8	10.0
9	14.9	6.7

the mechanism of this reaction involving Pd^{II} complexes. In the system $PdBr_2$—LiBr—MeCN—H_2O, palladium(II) bromide complexes most likely exist in the form of $Pd(AN)(CO)Br_2$, $Pd(CO)_2Br_2$, and $[Pd(CO)Br_3]^-$. Neutral complexes $Pd(AN)(CO)Br_2$ and $Pd(CO)_2Br_2$ exhibit high catalytic activity in the oxidation of CO.

Insertion of O_2 into the Pd—H bond in the palladium hydride complexes is the rate-limiting step of CO oxidation in the absence of co-catalyst (PcFe^{II}). The presence of iron(II) phthalocyaninate in the reaction system considerably decreases the activation energy of regeneration of the Pd^{II} complexes owing to more efficient activation of O_2. In this case the oxidation of palladium hydride complexes by iron superoxophthalocyaninate can follow two pathways that differ in fashion of hydride transfer.

The author expresses his gratitude to O. N. Temkin for valuable comments and advices. Calculations were carried out on computational facilities at the Joint Supercomputer Center of the Russian Academy of Sciences.

This work was financially supported by the Russian Foundation for Basic Research (Project No. 16-29-10674).

References

1. A. Klausner, J. D. Jentsch, in *Applied Homogeneous Catalysis with Organometallics Compounds*, Vol. 1, Eds B. Cornils, W. A. Herrmann, Wiley-VCH, Weinheim, 1996, p. 169.
2. O. N. Temkin, L. G. Bruk, *Oxidative Carbonylation — Homogeneous. Encyclopedia of Catalysis*, Vol. 5, Ed. I. T. Horvath, Willey-Int., Hoboken, 2003, p. 394.
3. O. N. Temkin, L. G. Bruk, *Kinet. Catal.* (*Engl. Transl.*), 2003, **44**, 601.
4. B. Gabrielle, G. Salerno, M. Costa, *Top. Organomet. Chem.*, 2006, **18**, 239.
5. L. G. Bruk, I. V. Oshanina, S N. Gorodskiy, *Ros. Khim. Zh.* [*Mendeleev Chem. J.*], 2006, **L**, Iss. 4, 103 (in Russian).
6. O. N. Temkin, G. K. Shestakov, Yu. A. Treger, In *Atsetilen: khimiya, mekhanizmy reaktsii, tekhnologiya* [*Acetylene: Chemistry, Reaction Mechanisms, and Technology*], Ed. O. N. Temkin, Khimiya, Moscow, 1991, 415 pp. (in Russian).
7. M. Beller, X.-F. Wu, *Transition Metal Catalyzed Carbonylation Reactions: Carbonylative Activation of C—X Bonds*, Springer, New York, 2013, p. 147.
8. O. N. Temkin, *Homogeneous Catalysis with Metal Complexes: Kinetic Aspects and Mechanisms*, Chichester, Wiley & Sons, 2012, 806 pp.
9. A. R. Elman, G. A. Korneeva, Yu. G. Noskov, V. N. Khan, E. Yu. Shishkina, V. M. Negrimovskiy, E. P. Ponomarenko, L. O. Kononov, L. G. Bruk, I. V. Oshanina, O. N. Temkin, S. G. Kuzmin, *Ros. Khim. Zh.* [*Mendeleev Chem. J.*], 2013, **LVII**, Iss. 5, 3 (in Russian).
10. L. G. Bruk, A. P. Kozlova, O. V. Marshakha, I. V. Oshanina, O. N. Temkin, O. L. Kaliya, *Russ. Chem. Bull.*, 1999, **48**, 1875.
11. L. G. Bruk, O. N. Temkin, I. V. Oshanina, A. P. Kozlova, E. V. Vorontsov, *Mol. Catal.*, 1995, **104**, 9.
12. I. V. Oshanina, S. I. Goloborod´ko, E. A. Robinova, I. N. Rusnak, S. A. Nikiforov, S. A. Prokhorov, O. N. Temkin, O. L. Kaliya, *Tonkie Khim. Tekhnol.* [*Fine Chem. Technol.*], 2019, **14**, No. 6, 76 (in Russian).
13. G. E. Efremov, E. A. Bovyrina, E. A. Katsman, R. S. Shamsiev, O. N. Temkin, *Russ. Chem. Bull.*, 2019, **68**, 1366.
14. D. N. Laikov, *Chem. Phys. Lett.*, 1997, **281**, 151.
15. D. N. Laikov, Yu. A. Ustynyuk, *Russ. Chem. Bull.*, 2005, **54**, 820.
16. J. P. Perdew, K. Burke, M. Ernzerhof, *Phys. Rev. Lett.*, 1996, **77**, 3865.
17. D. N. Laikov, *Chem. Phys. Lett.*, 2005, **416**, 116.
18. R. S. Shamsiev, I. E. Sokolov, F. O. Danilov, V. R. Flid, *Kinet. Catal.* (*Engl. Transl.*), 2019, **60**, 627.
19. S. Kozuch, J. M. L. Martin, *ACS Catal.*, 2011, **1**, 246.
20. A. Yu. Putin, E. A. Katsman, L. G. Bruk, *Russ. J. Phys. Chem. A* (*Engl. Transl.*), 2019, **93**, 222.
21. P. E. M. Siegbahn, *J. Phys. Chem.*, 1996, **100**, 14672.
22. B. J. Anderson, J. A. Keith, M. S. Sigman, *J. Am. Chem. Soc.*, 2010, **132**, 11872.
23. M. M. Konnick, S. S. Stahl, *J. Am. Chem. Soc.*, 2008, **130**, 5753.
24. N. Decharin, B. V. Popp, S. S. Stahl, *J. Am. Chem. Soc.*, 2011, **133**, 13268.
25. S. Sahu, D. P. Goldberg, *J. Am. Chem. Soc.*, 2016, **138**, 11410.

Received October 31, 2019;
accepted January 30, 2020